2600–2614 *Nucleic Acids Research, 2017, Vol. 45, No. 5* *Published online 19 December 2016*
doi: 10.1093/nar/gkw1275

Ribonucleotide incorporation by human DNA polymerase η impacts translesion synthesis and RNase H2 activity

Elisa Mentegari[1], Emmanuele Crespan[1], Laura Bavagnoli[1], Miroslava Kissova[1], Federica Bertoletti[1], Simone Sabbioneda[1], Ralph Imhof[2], Shana J. Sturla[3], Arman Nilforoushan[3], Ulrich Hübscher[2], Barbara van Loon[2] and Giovanni Maga[1,*]

[1]DNA Enzymology & Molecular Virology and Cell Nucleus & DNA replication Units, Institute of Molecular Genetics IGM-CNR, via Abbiategrasso 207, I-27100 Pavia, Italy, [2]Department of Molecular Mechanisms of Disease, University of Zürich, Winterthurerstrasse 190, CH-8057 Zürich, Switzerland and [3]Department of Health Sciences and Technology, ETH Zurich, Schmelzbergstrasse 9, CH-8092 Zürich, Switzerland

Received September 15, 2016; Revised December 05, 2016; Editorial Decision December 06, 2016; Accepted December 07, 2016

ABSTRACT

Ribonucleotides (rNs) incorporated in the genome by DNA polymerases (Pols) are removed by RNase H2. Cytidine and guanosine preferentially accumulate over the other rNs. Here we show that human Pol η can incorporate cytidine monophosphate (rCMP) opposite guanine, 8-oxo-7,8-dihydroguanine, 8-methyl-2'-deoxyguanosine and a cisplatin intrastrand guanine crosslink (cis-PtGG), while it cannot bypass a 3-methylcytidine or an abasic site with rNs as substrates. Pol η is also capable of synthesizing polyribonucleotide chains, and its activity is enhanced by its auxiliary factor DNA Pol δ interacting protein 2 (PolDIP2). Human RNase H2 removes cytidine and guanosine less efficiently than the other rNs and incorporation of rCMP opposite DNA lesions further reduces the efficiency of RNase H2. Experiments with XP-V cell extracts indicate Pol η as the major basis of rCMP incorporation opposite cis-PtGG. These results suggest that translesion synthesis by Pol η can contribute to the accumulation of rCMP in the genome, particularly opposite modified guanines.

INTRODUCTION

Several thousands to millions of ribonucleotides (rNMPs) are interspersed among the DNA bases of eukaryotic genomes (1). The presence of the 2′-OH group makes the sugar phosphate backbone of RNA 100 000-fold more prone to spontaneous hydrolysis than DNA. In addition, rNMPs induce B- to A-form transition in the double helix, potentially affecting protein-DNA interactions and the catalytic activity of DNA polymerases (Pols), topoisomerases and ligases and leading to further DNA damage (2). Thus, rNMPs in the genome constitute the most abundant DNA lesions in eukaryotic cells (3,4).

Deep sequencing studies in *Saccharomyces cerevisiae* found that cytosine and guanosine were the most abundant rNMPs in the genome (5–7). Their relative genomic abundance did not reflect their intracellular concentrations, with regard to their ratios with respect to those of adenosine and uracil, nor with respect to the relative G+C and A+T genomic content, suggesting that factors beside nucleotide pool concentrations and template sequence influence the accumulation of specific rNMPs in the genome.

Incorporation of rNMPs into the genome of proliferating cells, is predominantly mediated by the replicative Pols δ and ϵ (1). However, biochemical studies revealed that also several specialized repair Pols have poor sugar discrimination abilities (8–17), making rNMP incorporation during DNA repair or translesion synthesis (TLS) a likely event *in vivo*, given that the intracellular ribonucleoside triphosphates (rNTPs) concentrations are 100- to 1000-fold higher than those of deoxyribonucleoside triphosphates (dNTPs). In the context of TLS, rNMPs incorporation opposite a DNA lesion may delay subsequent removal of either the rNMPs or the damaged base, as recently was shown in the case of TLS over a 8-oxo-7,8-dihydroguanine (8-oxo-G) lesion by human Pols β and λ (16,18).

The process of TLS is mainly carried out by Y-family Pols η, ι and κ (19,20). One study (14) reported that human Pol ι has sugar discrimination values between 1000 and 6000 and can bypass abasic (AP) sites or 8-oxo-G lesions using rNTPs as substrates. On the contrary, yeast Pol η showed

*To whom correspondence should be addressed. Tel: +39 0382 546 354; Fax: +39 0382 422 286; Email: maga@igm.cnr.it
Present address: Barbara van Loon, Department of Cancer Research and Molecular Medicine, Norwegian University of Science and Technology, Erling Skjalgssons gt 1, N-7491 Trondheim, Norway.

limited rNMP incorporation for undamaged DNA templates or opposite a cyclobutane pyrimidine dimer (CPD) (21). A recent study that appeared during the preparation of the present work showed more robust rNMPs incorporation and elongation by human Pol η on both undamaged DNA and during TLS of a CPD or a 8-oxo-G lesion (17). The same study also provided the crystal structure of Pol η in complex with an incoming rCTP paired to a template 8-oxo-G, showing that the enzyme can accommodate both the C-8 OH group of the oxidized base and the 2′-OH group of the ribose sugar of the incoming nucleotide, due to its wide active site. However, whether TLS using rNMPs is a general feature of human Pol η, or it is limited to specific lesions, is currently not known.

Human Pol η is essential for TLS over CPDs, and its absence in humans causes a variant form of the genetic disease *Xeroderma pigmentosum* (XP-V) (20,22). Pol η is also involved in the bypass of other DNA lesions, such as 8-oxo-G and AP sites, and it plays an important role in bypassing the intrastrand crosslinks between two adjacent guanines caused by the anticancer drug cisplatin (cis-PtGG) (23). Thus, its ability to use rNTPs instead of dNTPs during TLS may have physiologically relevant consequences.

Once incorporated, rNMPs can be removed by the ribonucleotide excision repair (RER) pathway, which is initiated by the RNase H2 enzyme (4,24–26). This ribonuclease can specifically introduce a nick on the 5′-side of the DNA/RNA junction when 1 to 4 rNMPs are embedded in DNA. This cleavage subsequently triggers nick translation by the Pol δ holoenzyme, with the generation of a flap that is cut by the Flap endonuclease 1, resulting in the elimination of the RNA/DNA hybrid tract and re-synthesis of an intact DNA strand. Both the yeast *Schizosaccharomyces pombe* (27) and the *Escherichia coli* RNase H2 (18) were shown to incise cytidine monophosphate (rCMP) opposite 8-oxo-G. However, the impact of rNMP incorporation opposite damaged bases on the catalytic efficiency of human RNase H2 have not been carefully investigated yet.

In this work, we characterize the capacity of human Pol η to incorporate rNMPs opposite undamaged guanine or five different lesions: 8-oxo-G, 8-methyl-2′-deoxyguanosine (8-met-G), cis-PtGG, 3-methyldeoxycytidine (3-met-C) and an AP site. We also characterize the cleavage specificity of the human trimeric RNase H2 with respect to all four rNMP:dNMP base pairs, as well as its ability to cleave rCMP incorporated opposite 8-oxo-G, 8-met-G and cis-PtGG lesions. In addition we evaluated the effects in these reactions of the auxiliary protein proliferating cell nuclear antigen (PCNA) and also of DNA Pol δ interacting protein 2 (PolDIP2), which was shown to stimulate Pol η catalytic activity (28). Our results support the notion that Pol η can contribute to the genomic accumulation of rCMP, particularly opposite modified guanines.

MATERIALS AND METHODS

Chemicals

Deoxynucleotides were purchased from GeneSpin (Milan, Italy). Ribonucleotides were purchased by GE Healthcare (Uppsala, Sweden). Labeled [γ-^{32}P]ATP was purchased from Hartmann Analytic GmbH (Braunschweig, Germany). All other reagents were of analytical grade and purchased from Fluka or Merck.

Oligonucleotides

The 24mer oligonucleotide containing the cis-PtGG adduct was prepared and purified as described previously (29). All other DNA oligonucleotides were synthesized by Purimex (Grebenstein, Germany) and purified from polyacrylamide denaturing gels. When indicated, oligonucleotides were 5'-labeled with T4 polynucleotide kinase (New England Biolabs) and [γ-^{32}P]ATP, according to the manufacturer's protocol or directly synthesized as 5′-labeled with carboxyfluorescin (FAM) group. Each labeled primer was mixed to the complementary template oligonucleotide at 1:1 (M/M) ratio in the presence of 25mM Tris-HCl pH 8 and 50mM KCl, heated at 75°C for 10 min and then slowly cooled at room temperature.

A complete listing of sequences of the oligonucleotides used is given in the Supplementary Methods.

Enzymes and proteins

Recombinant human PCNA and PolDIP2 were expressed and purified as described (28). The bacterial clone for the expression of human Pol η was a kind gift from R. Woodgate (NIH, USA). Human recombinant Pol η was expressed and purified as described (30). The MIC1066 *E. coli* strain and the expression plasmid for the simultaneous expression of the three subunits of human RNase H2 were a kind gift of R. J. Crouch (National Institute of Child Health and Human development, Bethesda, MD, USA). The heterotrimeric human recombinant RNase H2 was expressed and purified as described (31), with the following modifications: cells were lysed for 30 min on ice in 20 mM KPO4 buffer pH 7.4, 300 mM NaCl, 30 mM Imidazole, 10 mg ml^{-1} lysozyme, 0.05% phenylmethylsulfonyl fluoride and protease inhibitors. The lysate was sonicated and cleared by ultracentrifugation at 38 000 rpm in a Ti70 Beckman rotor. The cleared lysate was loaded onto a FPLC-NiNTA column (G&E Healthcare) equilibrated in 20 mM KPO4 buffer pH 7.4, 300 mM NaCl, 30 mM imidazole, 5% glycerol. The protein was eluted with a 30–500 mM linear gradient of imidazole in the equilibration buffer. The fractions containing the enzyme in 20% glycerol were stored separately in liquid nitrogen.

Cell lines and culturing conditions

XP-V patient-derived XP30R0 fibroblast cells transformed with simian virus 40 were a gift from Alan Lehman (University of Sussex, Brighton, UK). XP-V cells were grown in a humidified 5% CO_2 atmosphere in Dulbecco's modified Eagle's medium containing GlutaMAX-I supplemented with 10% fetal bovine serum and 100 U/ml penicillin–streptomycin (all obtained from Gibco, Invitrogen). To complement XP-V cells, human Pol η mammalian expression vector pJRM56 (kindly provided by Roger Woodgate, NIH, USA) was used. pJRM56 or empty pcDNA 3.1 (Invitrogen) constructs were transiently transfected into XP-V cells using lipofectamine (Invitrogen) according to man-

ufacturers protocol. Alternatively XP30RO cells stably expressing eGFP-Polη were used (32,33). Cells were harvested 48 h respectively after transfection or seeding and whole-cell extract (WCE) were prepared. Cells were harvested 48 h after the transfection and WCE prepared.

Cell extracts and western blot

Cell extracts were prepared as described (34). Proteins were separated on 10% Bis-Tris poly-acrylamide gels and transferred to Immobilon-FL membrane (Millipore) for immunoblotting analysis. Primary antibodies against Pol η (Abcam), Pol β (custom made antibody) and Tubulin (Sigma) were detected using infrared dye-conjugated secondary antibodies (LI-COR Biosciences). For signal visualization the Odyssey Scanner (LI-COR Biosciences) was used.

Enzymatic assays

All reactions were in a 10 μl final volume. Pol η reaction buffer: 40 mM Tris pH 8, 1 mM dithiotreitol, 0.25 mg/ml bovine serum albumin (BSA). Mg^{2+} was included at 5 mM, unless otherwise stated in the figures or figure legends. RNase H2 reaction buffer: 50 mM Tris-HCl pH 8.5, 25 mM NaCl, 50 μg ml^{-1} BSA, 1 mM 2-mercaptoethanol, 1% glycerol, 5 mM Mg^{2+}. Enzymes and DNA substrates concentrations are indicated in the figures or figure legends. Reactions were incubated at 37°C for 5 min, unless otherwise stated in the figures or figure legends. For denaturing gel analysis of the DNA products, the reaction mixtures were stopped by addition of standard denaturing gel loading buffer (95% formamide, 10 mM ethylenediaminetetraacetic acid, xylene cyanol and bromophenol blue), heated at 95°C for 5 min and loaded on a 7 M urea 12% polyacrylamide (PA) gel. The reaction products were analyzed by using Molecular Dynamics Phosphoimager (Typhoon Trio, GE Healthcare) and quantified by the program Image Quant.

Kinetic analysis

Due to the highly distributive nature of the reaction and the relatively low efficiency of rNTP incorporation, the Pols and the DNA substrate were used at similar concentrations. This implies that, at equilibrium, the concentration of the binary enzyme-DNA complex does not approximate the total enzyme concentration, but there is always a fraction of enzyme not bound to the DNA substrate, which does not participate in catalysis. Thus, in order to account for the fraction of enzyme not bound to the DNA substrate at equilibrium, the variation of the nucleotide incorporation rates (v) as a function of the nucleotide substrate concentration was fitted to the modified Briggs-Haldane equation:

$$v = \frac{k\text{cat}\, E_0 S}{(S \cdot a) + (K_d \cdot b)} \quad (1)$$

where k_{cat} is the apparent catalytic rate, E_0 is the input enzyme concentration, S is the variable nucleotide substrate concentration, K_d is the apparent equilibrium dissociation constant of the nucleotide substrate from the catalytically active ternary complex, a and b are two constants, whose values were kept fixed during the computer fitting and were calculated from the expressions:

$$a = \frac{1}{1 + \frac{Kd}{K'}} \quad (2)$$

$$b = \frac{1}{\left(1 + \frac{K'}{S}\right)} \quad (3)$$

where K_d is the same as in Equation (1), K' is the apparent dissociation constant for binding to the DNA substrate and S' is the concentration of DNA use in each experiment. The value of K' used for the fitting process for Pol η was 11 nM (35).

In the case of RNase H2, the apparent initial velocities were plotted as a function of the DNA substrate concentrations and fitted to the Michaelis-Menten equation:

$$v = \frac{k\text{cat}\, E_0 S}{K_M + S} \quad (4)$$

here k_{cat} is the apparent catalytic rate, E_0 is the input enzyme concentration, S is the variable DNA substrate concentration, K_M is the apparent Michaelis constant.

Fitting was obtained with the GraphPad Prism 3.0 computer program.

Electronic image manipulation

Linear transformations have been applied in some instance to the whole images using the exposure/brightness filters of Adobe Photoshop CS6 with the sole purpose of reducing excessive background. No masking/enhancement was applied to any specific feature of the images. Solid lines identify different portions of the same gel brought next for clarity of presentation.

RESULTS

Incorporation of ribonucleotides by human Pol η

Human Pol η was incubated in the presence of a mixture of the four rNTPs or dNTPs, each present at its average intracellular concentration. Incorporation was measured as a function of increasing concentrations of Mg^{2+} or Mn^{2+} cofactors. As shown in Figure 1A, Pol η incorporated multiple rNMPs in the presence of physiological concentration (5 mM) of Mg^{2+} (Figure 1A, lane 9), but also at Mn^{2+} concentrations as low as 0.1 mM, even displaying more robust activity than with Mg^{2+}, at relatively high Mn^{2+} concentrations (0.5–1 mM) (Figure 1A, lanes 4 and 5). The 5 mM Mg^{2+} concentration was then used for all subsequent experiments. Pol η showed remarkable fidelity, being able to significantly incorporate rCMP only opposite an undamaged guanine (Figure 1B). When dCTP or rCTP were titrated into the reaction, robust incorporation of both nucleotides was observed opposite the template G, along with some misincorporation events leading to a +2 product (Figure 1C, lanes 4–7 and 12–15). The kinetic parameters for rCMP versus dCMP incorporation opposite a normal G are summarized in Table 1. On this template, the discrimination factor for deoxy- versus ribonucleotide incorporation by Pol η

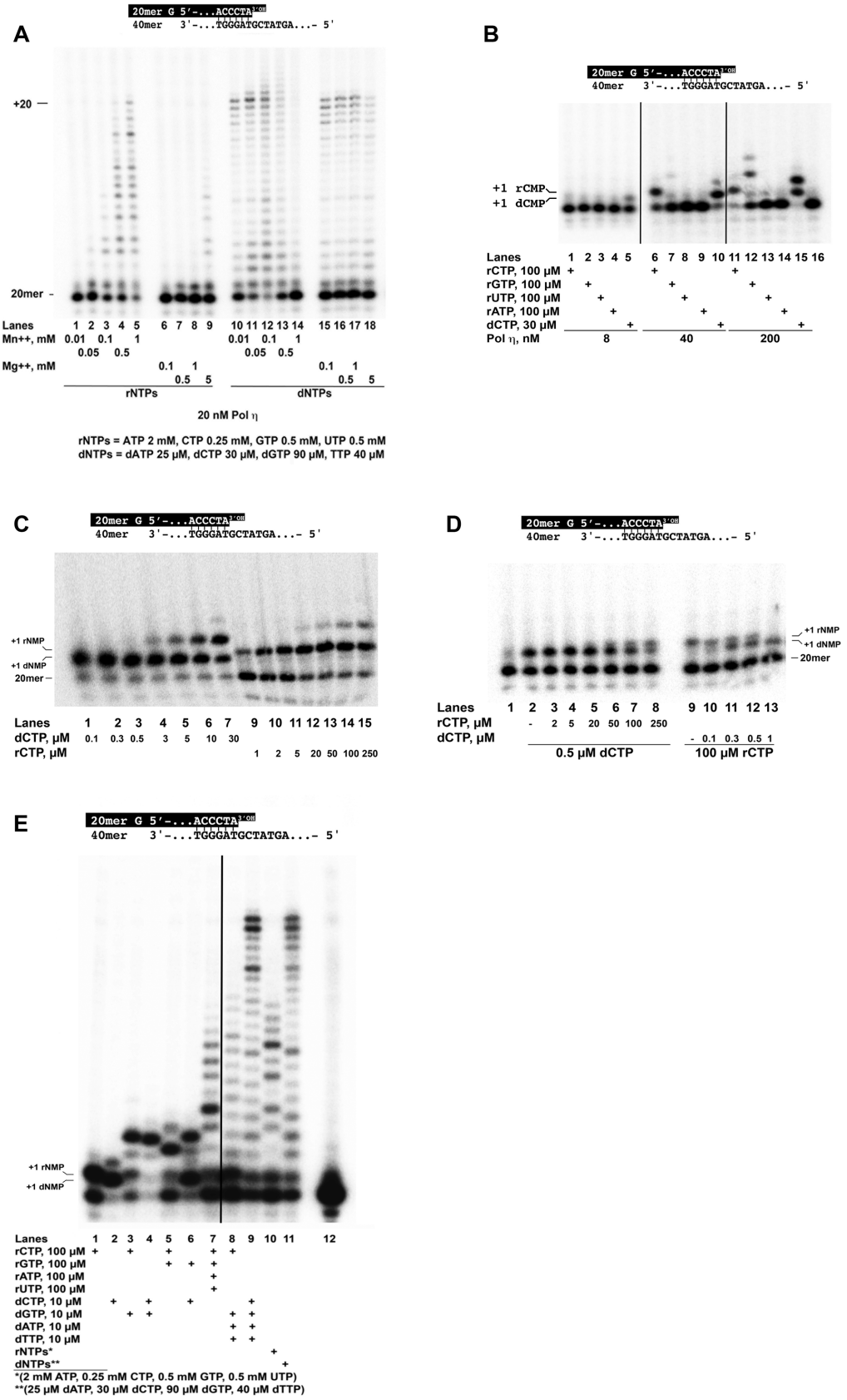

Figure 1. Incorporation and elongation of ribonucleotides by human Pol η. The sequence of the 5′ ^{32}P-labeled 20/40mer substrate (50 nM) used in all the experiments is indicated on top of each panel. (**A**) Pol η (20 nM) was incubated in the presence of non-equimolar mixtures of rNTPs (lanes 1–9) or dNTPs

was 400. Since the products arising from rCMP incorporation had a different electrophoretic mobility with respect to those due to dCMP incorporation, it was possible to simultaneously visualize both incorporation events in the same reaction. Indeed, titrating rCTP in the reaction, in the presence of fixed amounts of dCTP, led to the accumulation of the +1 rCMP product with concomitant reduction of the +1 dCMP product (Figure 1D, lanes 3–8). The same pattern was observed in the reciprocal experiment, i.e. titrating dCTP while keeping rCTP fixed (Figure 1D, lanes 9–13). These results confirmed that dCTP and rCTP can compete for incorporation opposite G. Comparable amounts of either products were observed at a rCTP/dCTP (M/M) ratio between 500 (Figure 1D, lane 8) and 300 (Figure 1D, lane 11), in agreement with the selectivity value derived from the kinetic analysis.

Pol η can synthesize hybrid DNA/RNA chains

Next, different combinations of the four deoxy- or ribonucleotides were tested, according to the template sequence. As shown in Figure 1E, after rCMP incorporation at position +1, Pol η was able to efficiently elongate by incorporating either deoxy- (Figure 1E, lane 3) or ribo-GMP (lane 5) opposite C at position +2. Similarly, efficient elongation was observed starting from a dCMP-terminated primer, with either deoxy- or ribo-GMP (Figure 1E, lanes 4 and 6). Long products were synthesized by Pol η when provided with all four rNTPs at equimolar (Figure 1E, lane 7) or physiological (lane 10) concentration ratios. Comparable products were observed when rCTP was provided in combination with the three remaining dNTPs (Figure 1E, lane 8). These products, however, were shorter than those synthesized in the presence of dNTPs only (Figure 1 E, lanes 9 and 11). Overall, these results indicated that Pol η can efficiently elongate rNMP-terminated primers, synthesizing both RNA and RNA/DNA polynucleotide chains.

Translesion synthesis of 8-oxo-G by Pol η with ribonucleotides

Pol η can perform faithful bypass of 8-oxo-G, inserting dCMP. When rCTP was provided in the reaction, robust incorporation opposite 8-oxo-G was observed for both a 1-nt gapped (Figure 2A, lanes 1–6) or an open primer/template (Figure 2B, lanes 1–5). The kinetic parameters for rCMP and dCMP incorporation opposite 8-oxo-G are summarized in Table 1. The selectivity of Pol η for dCMP versus rCMP incorporation opposite the lesion was increased 3.5-fold, with respect to a normal G, showing a value of 1428. Pol η could also incorporate both dAMP and rAMP, opposite the lesion (Figure 2C). The selectivity for dAMP versus rAMP was in the order of 3800, while the preference for dCMP versus rAMP incorporation was 12 700 (Table 1). Interestingly, the fidelity of lesion bypass was increased with rNTPs relative to dNTPs, with a 3.3-fold preference for dCMP versus dAMP incorporation and an 8.9-fold preference for rCMP versus rAMP incorporation, respectively (Table 1). These values were also in agreement with those reported in a recent study (17). When all four dNTPs or rNTPs were provided, Pol η could perform efficient TLS (Figure 2D, compare lane 1 with lane 5). The products synthesized in the presence of rNTPs were sensitive to RNase treatment (Figure 2D, lane 3), confirming that they were authentic RNA chains. These results indicated that Pol η can synthesize RNA chains as a result of TLS past an 8-oxo-G lesion.

Pol η bypasses 8-met-G, but not 3-met-C with ribonucleotides

We extended our investigation of Pol η bypass to the 3-met-C and 8-met-G alkylation lesions. As shown in Figure 3A, Pol η incorporated all four dNMPs opposite 3-met-C or 8-met-G (Figure 3A, lanes 2–5; 11–14). On the contrary, while none of the rNMPs was incorporated opposite 3-met-C (Figure 3A, lanes 1–9), robust rCMP incorporation was observed opposite 8-met-G (lane 16). Titration of dCTP or rCTP in the reaction revealed the accumulation of the expected +2 product (Figure 3B), indicating efficient TLS by Pol η with both deoxy- and ribonucleotides. The kinetic parameters for 8-met-G bypass are summarized in Table 1. The selectivity for dCMP versus rCMP incorporation by Pol η opposite 8-met-G was 693, which is only slightly higher than the selectivity measured opposite a normal G. To the best of our knowledge, this is the first report of bypass of the 8-met-G lesion by a human pol with rNTPs.

Next, the effect of the auxiliary proteins PCNA and PolDIP2 was tested. PCNA did not stimulate rCMP incorporation opposite 8-met-G by Pol η (Figure 3C, compare lanes 1–4 with lanes 7–10). On the other hand, a significant stimulation was observed in the presence of PolDIP2 (Figure 3C, lanes 11–14). Kinetic analysis showed that PolDIP2 increased the apparent catalytic efficiency (k_{cat}/K_M) for rCMP incorporation by 6-fold, lowering the selectivity value of Pol η for dCMP versus rCMP incorporation to 111 (Table 1). PolDIP2 stimulated TLS by Pol η past 8-met-G also when all four dNTPs or rNTPs were provided to the reaction at their average physiological concentrations (Figure 3 D). However, the length of the RNA chains synthesized were limited to about 5 nt (Figure 3D, lanes 5–8), while full length products were detected with dNTPs (Figure 3D, lanes 1–4). When PCNA was added in the reaction in a molar excess with respect to PolDIP2, TLS by Pol η with rNTPs was partially inhibited (Supplementary Figure S1A, lane 4). However, this effect was abolished when the PolDIP2 concentration was increased (lane 8), suggesting a

←

(lanes 10–18) and different amounts of Mn2+ (lanes 1–5; 10–14) or Mg 2+ (lanes 6–9; 15–18). The final concentrations of the individual rNTPs and dNTPs are indicated on the bottom of the panel. (**B**) Increasing amounts of Pol η were titrated in the presence of fixed concentrations of each individual rNTP (lanes 1–4; 6–9; 11–14) or dCTP (lanes 5, 10, 15). Lane 16, control reaction in the absence of nucleotides. (**C**) Pol η (40 nM) was tested in the presence increasing concentrations of dCTP (lanes 1–7) or rCTP (lanes 9–15). **D**. Pol η (20 nM) was tested in the presence of a fixed dose of dCTP and increasing concentrations of rCTP (lanes 2–8) or a fixed dose of rCTP and increasing concentrations of dCTP (lanes 9–13). Lane 1, control reaction in the absence of nucleotides. (**E**) Pol η (40 nM) was tested in the presence of various combinations of dNTPs or rNTPs. Lane 12, control reaction in the absence of nucleotides.

Table 1. Kinetic parameters for nucleotide incorporation opposite G, 8oxoG or 8metG by Pol η

Nucleotide	K_M, μM[a]	k_{cat}, min^{-1}	k_{cat}/K_M M^{-1} s^{-1}	f_{rel}[b] (dCTP/rCTP)	f_{rel} (dCTP/dATP)	f_{rel} (dCTP/rATP)	f_{rel} (rCTP/dATP)	f_{rel} (rCTP/rATP)
39/100mer G								
dCTP	0.20 ± 0.05	1.9 ± 0.05	1.60×10^5	400	n.a.	n.a.	n.a.	n.a.
rCTP	15 ± 0.3	0.40 ± 0.1	0.40×10^3					
39/100mer 8oxoG								
dCTP	0.50 ± 0.02	1.8 ± 0.01	0.60×10^5	1428	3.30	12 765		
rCTP	117 ± 4	0.30 ± 0.01	42				2.30×10^{-3}	8.90
dATP	0.30 ± 0.01	0.32 ± 0.01	0.18×10^5					
rATP	247 ± 5	0.07 ± 0.02	4.70					
39/72mer 8metG								
dCTP	2.70 ± 0.1	1.10 ± 0.02	6.80×10^3	693	n.a.	n.a.	n.a.	n.a.
rCTP	187 ± 3	0.11 ± 0.03	9.80					
rCTP + PolDIP2	100 ± 2	0.37 ± 0.04	61	111				
18/24mer GG								
dCTP	0.30 ± 0. 3	2.50 ± 0.2	1.40×10^5	546	n.a.	n.a.	n.a.	n.a.
rCTP	26 ± 0.5	0.40 ± 0.2	256					
18/24mer cis-Pt								
dCTP	1.50 ± 1	1.20 ± 0.1	1.30×10^4	1212	n.a.	n.a.	n.a.	n.a.
rCTP	113 ± 5	0.07 ± 0.01	11					

[a]Kinetic parameters have been calculated as indicated in the 'Materials and Methods' section. Values are the means of three independent experiments ±S.D.
[b]Relative incorporation frequency, f_{rel} was calculated as the ratio between the k_{cat}/K_M values for the indicated nucleotide pairs.

possible competition between PCNA and Pol η for binding to PolDIP2.

Pol η bypasses cis-PtGG but not an abasic site with ribonucleotides

Pol η is the main enzyme involved in the bypass of the intrastrand guanine crosslinks caused by the anticancer drug cisplatin (cis-PtGG) (36). When tested in the presence of each of the four rNTPs, Pol η was capable of incorporating rCMP opposite the lesion (Figure 4A, lane 10). The products observed with rGTP and rUTP as substrates resulted from the incorporation of dNTPs contaminating the commercial preparation used, as judged by their electrophoretic mobility, which was similar to those of products obtained with dCTP as substrate (Figure 4A, compare lanes 8, 9 with lane 7; Supplementary Figure S1B and C). Interestingly, the incorporation of rCMP was largely limited to the +1 product (Figure 4A, lane 10), corresponding to incorporation opposite the first guanine (termed 3′-G, according to the template strand orientation) of the adduct, similar to what has been observed for the insertion of non-canonical dNTPs opposite Pt-GG by Pol η (29), while dCMP was correctly incorporated opposite both guanines, yielding the expected +2 product (Figure 4A, lane 2). Titration of dCTP (Figure 4B) or rCTP (Figure 4C) into the reaction confirmed that rCMP incorporation was limited to opposite the 3′-G of cisPt-GG (Figure 4C, lanes 9–4). PolDIP2 stimulated rCMP (Figure 4D) and dCMP (Figure 4E) incorporation by Pol η opposite cis-PtGG, but even in the presence of PolDIP2, rCMP incorporation was limited to the first position (Figure 4 D, lanes 5–13). When a primer/template bearing a rCMP opposite the 3′-G of the lesion was tested, only dCMP, but not rCMP, was incorporated opposite the 5′-G (Figure 4F). Interestingly, when a primer/template with a dCMP opposite the 3′-G was used, no incorporation of rCMP was observed either (Figure 4G). Overall, these results indicated that bypass of a cis-PtGG adduct by Pol η can lead to incorporation of rCMP opposite the first guanine (3′-G) only. The bypass, however, can be subsequently completed by incorporating dCMP opposite the 5′-G. The selectivity for dCMP versus rCMP incorporation opposite the two guanines on the undamaged template was 546, similar to the one observed on the template with a single guanine (Table 1). This selectivity was increased to about 1200, opposite the 3′-G of cisPt-GG, a value similar to the one observed for 8-oxo-G (Table 1). In a competition experiment, dCTP was titrated in the presence of the cisPt-GG template and fixed amounts of rCTP, resulting in the accumulation of the +1 dCMP product with concomitant reduction of the +1 rCMP product (Figure 4 H, lanes 2–6). The same pattern was observed in the reciprocal experiment, i.e. titrating rCTP while keeping dCTP fixed (Figure 4H, lanes 7–10). These results confirmed that dCTP and rCTP can compete for incorporation opposite the 3'-G of a cisPt-GG adduct. Comparable amounts of either products were observed at a rCTP/dCTP (M/M) ratio of 1/1000 (Figure 4H, lanes 4 and 10), in agreement with the selectivity value derived from the kinetic analysis (Table 1). Simultaneous incorporation of rCMP and dCMP opposite the lesion was also observed in a similar competition experiment carried out with XP-V/η extracts (Figure 4I, lane 6), suggesting that rCMP incorporation opposite the cisPt-GG lesion by Pol η can also occur in a cellular context.

Finally, when tested in the presence of an AP site, Pol η was unable to significantly incorporate rNMPs opposite the lesion (Supplementary Figure S1D, lanes 1–4), even in the presence of PolDIP2 (lanes 7–10), with the exception of a very weak incorporation of rCMP (Supplementary Figure S1F, lane 10), while it efficiently bypassed the lesion with either dATP or all four dNTPs (Supplementary Figure S1D, lanes 5, 6, 11 and 12).

Ribonucleotide-mediated lesion bypass in XP-V cell extracts

The rCMP incorporation opposite 8-oxo-G was measured in extracts from XP-V cells lacking Pol η, in comparison with the same XP-V cell line complemented with ectopic expression of human Pol η (XP-V/h). As shown in Supplementary Figure S1E, TLS of 8-oxo-G with rCMP was detected in both XP-V and XP-V/η extracts (lanes 1–3). When this activity was normalized to the total Pol activity (measured as incorporation of dCMP opposite a normal G, Supplementary Figure S1F), rCMP incorporation was reduced

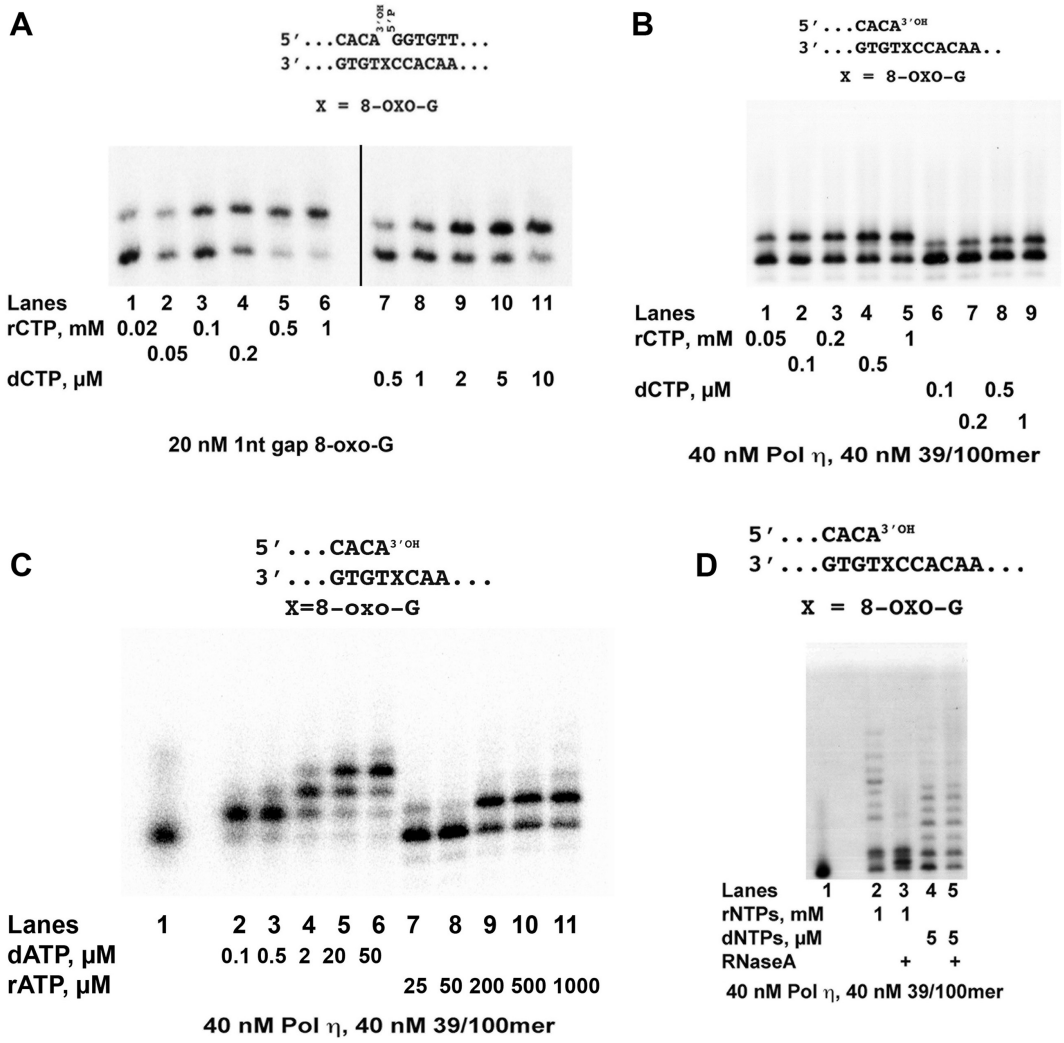

Figure 2. Translesion synthesis of 8-oxo-G by Pol η with ribonucleotides. The sequences of the 5′ ^{32}P-labeled DNA substrates used are indicated on top of each panel. (**A**) Pol η (40 nM) was incubated with the 1-nt gapped 8-oxo-G template, in the presence of increasing concentrations of rCTP (lanes 1–6) or dCTP (lanes 7–11). (**B**) Pol η was incubated with the 39/100-mer 8-oxo-G template, in the presence of increasing concentrations of rCTP (lanes 1–5) or dCTP (lanes 6–9). (**C**) Pol η was incubated with the 39/100-mer 8-oxo-G template, in the presence of increasing concentrations of dATP (lanes 2–6) or rATP (lanes 7–11). Lane 1, control reaction in the absence of nucleotides. (**D**) Pol η was incubated with the 39/100-mer 8-oxo-G template, in the presence of all four rNTPs (lanes 2, 3) (1 mM each, final concentration) or dNTPs (lanes 4, 5) (5 μM each, final concentration). 2 Units of RNaseA (lanes 3, 5) or buffer (lanes 2, 4) were added after 10 min and the incubation continued for additional 5 min. Lane 1, control reaction in the absence of nucleotides.

by about 25% in the absence of Pol η (Supplementary Figure S1G). The majority of rCMP incorporation opposite 8-oxo-G has been shown to be carried out by Pol β (16). Western blot analysis of the extracts confirmed that both Pol β and Pol η were present in the extracts (Supplementary Figure S1H). Thus, the apparently modest contribution of Pol η to rCMP incorporation opposite 8-oxo-G, could be explained by the competition of Pol β. On the other hand, when the extracts were tested with the cis-PtGG template, bypass was observed only in XP-V/η cells, with either dCMP or rCMP (Supplementary Figure S1I), in agreement with the notion that Pol η contributes most to TLS past this lesion. Collectively, these data suggest that the frequency of rNMP incorporation opposite a certain lesion is a function of (i) the type of TLS pols potentially acting on that lesion, (ii) their sugar selectivity and (iii) their relative affinity for the lesion.

Cleavage of rCMP opposite normal or damaged guanines by human RNase H2

In a 1993 report of the first purification from mammalian cells of the enzyme later identified as RNase H2, Eder *et al.* showed that the efficiency of the enzyme depended on the identity of the base pair being cleaved (37). To verify this property, we expressed and purified the recombinant human trimeric RNase H2 (Supplementary Figure S3A) and tested it with all four ribo-to-deoxynucleoside base pairs. Time course experiments were performed with increasing amounts of the 40/40mer ds DNA oligonucleotide substrates, bearing either a rC:dG, rG:dC, rA:dT or rU:dA pair at a specific position. The strand containing the single rNMPs was 5′-labeled so that after cleavage by RNase H2, products of a defined length were generated and resolved by sequencing gel electrophoresis. Representative experi-

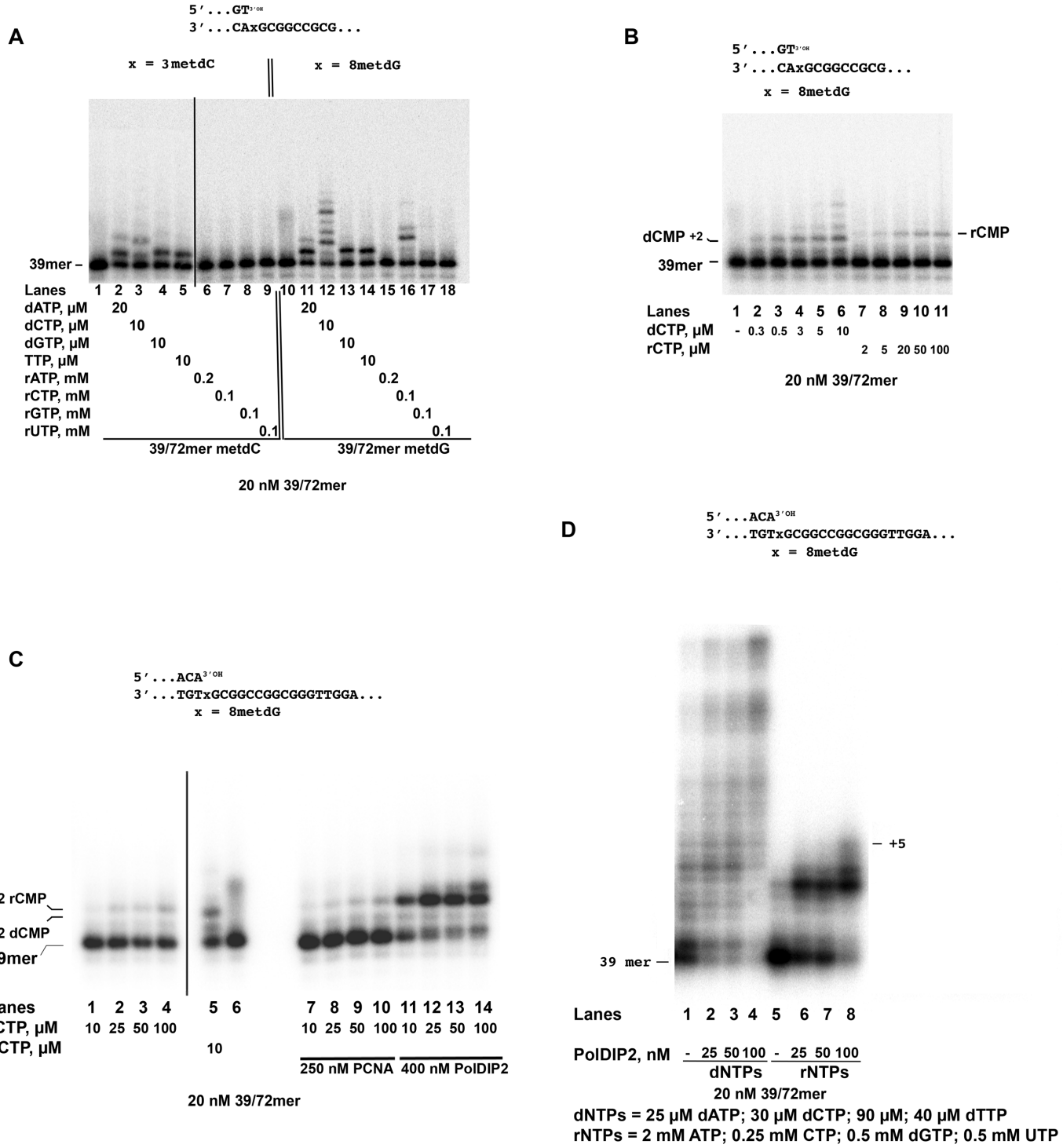

Figure 3. Pol η bypass of 8-met-G and 3-met-C with ribonucleotides. The sequences of the 5′ ^{32}P-labeled DNA substrates used are indicated on top of each panel. (**A**) A total of 20 nM Pol η was incubated in the presence of the 3-met-C (lanes 1–9) or 8-met-G (lanes 10–18) 39/72mer substrates and a fixed concentration of each dNTP (lanes 2–5; 11–14) or rNTP (lanes 6–9; 15–18). Lanes 1 and 10, control reactions without nucleotides. (**B**) 20 nM Pol η was incubated with the 8-met-G substrate, in the presence of increasing concentrations of dCTP (lanes 2–6) or rCTP (lanes 7–11). Lane 1, control reaction in the absence of nucleotides. (**C**) 20 nM Pol η was incubated with the 8-met-G substrate, in the presence of rCTP (lanes 1–4; 7–14) or dCTP (lane 5) and in the absence (lanes 1–5) or in the presence of PCNA (lanes 7–10) or PolDIP2 (lanes 11–14). Lane 6, control reaction in the absence of nucleotides. (**D**) A total of 20 nM Pol η was incubated with the 8-met-G substrate, in the presence of non-equimolar mixtures of dNTPs (lanes 1–4) or rNTPs (lanes 5–8) and in the absence (lanes 1, 5) or in the presence of increasing concentrations of PolDIP2 (lanes 2–4; 6–8). The final concentrations of the individual rNTPs and dNTPs are indicated on the bottom of the panel.

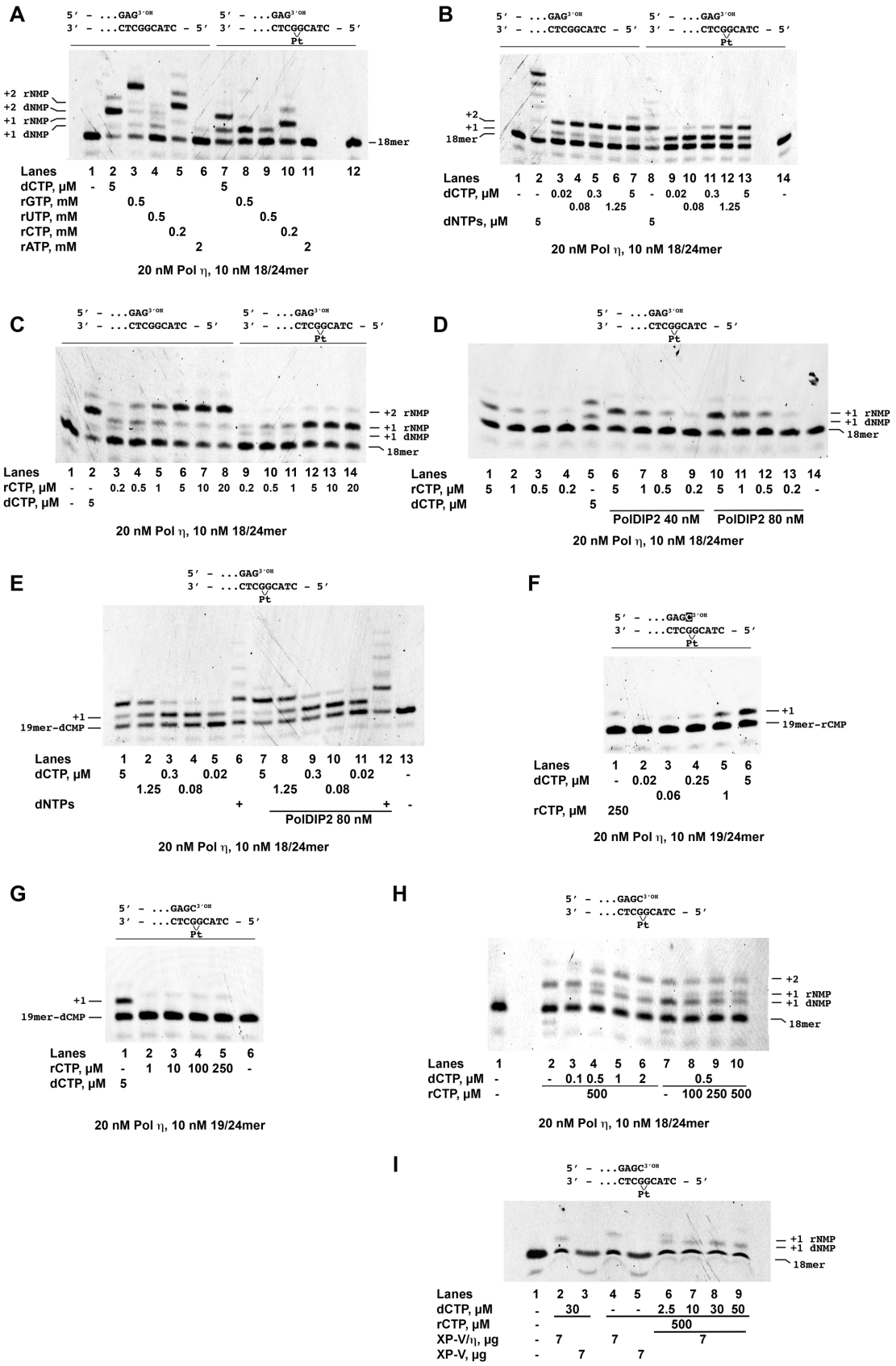

Figure 4. Pol η bypass of cis-PtGG and abasic site with ribonucleotides. The 5′ FAM-labeled DNA substrates used are indicated on top of each panel. (**A**) Pol η was incubated with the undamaged (lanes 1–6) or the cis-PtGG (lanes 7–12) templates, with dCTP (lanes 5, 7) or each rNTP (lanes 3–6; 8–11).

Table 2. Kinetic parameters for RNase H2 cleavage of different ribo-/deoxynucleoside basepairs

Basepair	K_M (nM)[a]	k_{cat} (min^{-1})	k_{cat}/K_M (M^{-1}, s^{-1})	efficiency (-fold)
rA:dT	10 ± 3	6.7 ± 0.2	11×10^6	6.1
rU:dA	12 ± 2	3.1 ± 0.5	4.3×10^6	2.4
rC:dG	8 ± 2	0.9 ± 03	1.8×10^6	1
rG:dC	27 ± 5	1.2 ± 0.3	0.7×10^6	0.4

[a]Kinetic parameters have been calculated as indicated in the 'Materials and Methods' section. Values are the means of four independent experiments ±S.D.

ments are shown in Supplementary Figure S2A–D, while the kinetic parameters are summarized in Table 2. Human RNase H2 had a strong preference for rA:dT cleavage, followed by rU:dA. Interestingly, rC:dG and rG:dC pairs were cleaved with a 6-fold and 15-fold reduced efficiency with respect to rA:dT. RNase H2 subunit H2B contains a PCNA-binding domain and PCNA has been shown to interact with RNase H2 and direct it to the DNA substrate. We therefore tested whether PCNA could rescue the reduced catalytic activity of human RNase H2 with rC- or rG-containing substrates. As shown in Supplementary Figure S2B and C, however, PCNA did not stimulate rC:dG or rG:dC cleavage by RNase H2.

Next, we evaluated whether rCMP paired to a damaged guanine may affect RNase H2 cleavage. RNase H2 showed a 3.4-fold reduced efficiency in removing rCMP when it was opposite 8-oxo-G versus G (Figure 5A and B). On the other hand, no differences were seen in cleavage efficiency between rC:dG and rC:8metG pairs (Figure 5C and D). RNase H2 exhibited reduced cleavage efficiency of rCMP opposite both the 3′-G and 5′-G of cis-PtGG relative to the controls (Supplementary Figure S2D). Since rCMP incorporation by Pol η can occur only opposite the 3′-G (see Figure 4), we better characterized RNase H2 cleavage at this position (Figure 5E). Quantification of the results indicated a 3.8-fold reduced cleavage efficiency by RNase H2 when rCMP was opposite the 3′-G of a cis-PtGG lesion, relative to it being opposite an undamaged guanine at the same position (Figure 5F). Overall, these results indicated that rCMP opposite an undamaged guanine is already less efficiently cleaved by RNase H2, and incorporation of rCMP as a result of TLS can further reduce the efficiency of its removal by RNase H2.

DISCUSSION

In the present study, we addressed the possible consequences of rNMPs incorporation by human Pol η in the context of TLS of five different lesions (8-oxo-G, 8-met-G, 3met-C, cis-PtGG and AP site), by studying not only the incorporation by Pol η *per se*, but also the subsequent cleavage of the incorporated rNMPs by human RNase H2 and the impact of auxiliary proteins in the TLS process. In fact, the incorporation of rNMPs in the context of TLS would result in an aberrant base pair, in which the rNMP is placed opposite the original DNA lesion. As a result, the cell will need to act upon *two paired lesions*: the rNMP on the newly synthesized strand and the original lesion on the template strand.

We found that human Pol η, at physiological concentrations of Mg^{2+} and rNMPs, has robust DNA-dependent RNA Pol activity, being able to synthesize several nucleotides-long RNA chains, either on undamaged DNA or during TLS. Thus, Pol η behaves differently from Pols β and λ, whose activity is limited to the incorporation of one or two rNMPs (16), but similar to the X-family Pol μ (9,13) or the Y-family Pol ι (14).

These results suggest that Pol η may amplify the number of rNMPs incorporated into the genome, for example if TLS occurs on a gapped DNA intermediate behind the replication fork, as has been suggested. Such long RNA chains may represent an additional challenge to the cell. It has been observed that in *S. cerevisiae*, deletion of the Rad30 gene (encoding yeast Pol η) reduces the toxic effects due to inactivation of RNaseH1 and RNase H2, both required to remove RNA chains longer than 4 nt (38). The same studies indicated Pol ζ as the TLS enzyme essential to relieve the cells from the stress due to excessive rNMPs accumulation in the genome. Replicative pols δ and ε can bypass only a limited number (< 4) of rNMPs in the template strand (39,40), while Pol ζ can easily copy a template containing multiple rNMPs (38). These findings, together with studies on yeast strains expressing a mutant Pol η with increased ability to incorporate rNMPs (21), support the hypothesis that Pol η leads to the accumulation of long stretches of RNA in the genome in cells lacking RNase H2

←

Lanes 1, 12, control reactions without nucleotides. (**B**) Pol η was incubated with the undamaged (lanes 1–7) or the cis-PtGG (lanes 8–14) templates, in the presence of dNTPs (lanes 2, 8) or dCTP (lanes 3–7; 9–13). Lanes 1, 14, control reactions without nucleotides. (**C**) Pol η was incubated with the undamaged (lanes 1–8) or the cis-PtGG (lanes 9–14) templates, in the presence of rCTP (lanes 3–14). Lane 1, control reaction without nucleotides. Lane 2, control reaction with dCTP. (**D**) Pol η was incubated with the cis-PtGG template in the presence of rCTP (lanes 1–4; 6–13) and in the absence (lanes 1–4) or in the presence of PolDIP2 (lanes 6–13). Lane 5, control reaction with dCTP. Lane 14, control reaction without nucleotides. (**E**) Pol η was incubated with the cis-PtGG template in the presence of dNTPs (lanes 6, 12) or dCTP (lanes 1–5; 7–11) and in the absence (lanes 1–6) or in the presence of PolDIP2 (lanes 7–12). Lane 13, control reaction without nucleotides. (**F**) Pol η was incubated with the cis-PtGG template bearing a rCMP opposite the 3′-G of the lesion, in the presence of rCTP (lane 1) or dCTP (lanes 2–6). (**G**) Pol η was incubated with the cis-PtGG template bearing a dCMP opposite the 3′-G of the lesion, in the presence of dCTP (lane 1) or rCTP (lanes 2–5). Lane 6, control reaction without nucleotides. (**H**) Pol η (20 nM) was tested in the presence of a fixed dose of rCTP and increasing concentrations of dCTP (lanes 2–6) or a fixed dose of dCTP and increasing concentrations of rCTP (lanes 7–10). Lane 1, control reaction in the absence of nucleotides. (**I**) XP-V (lanes 3, 5) or XP-V/η (lanes 2, 4, 6–9) extracts, were incubated with the cis-PtGG template in the presence of dCTP alone (lanes 2, 3), rCTP alone (lanes 4, 5) or both nucleotides at different M/M ratios (lanes 6–9). Lane 1, control reaction in the absence of extracts.

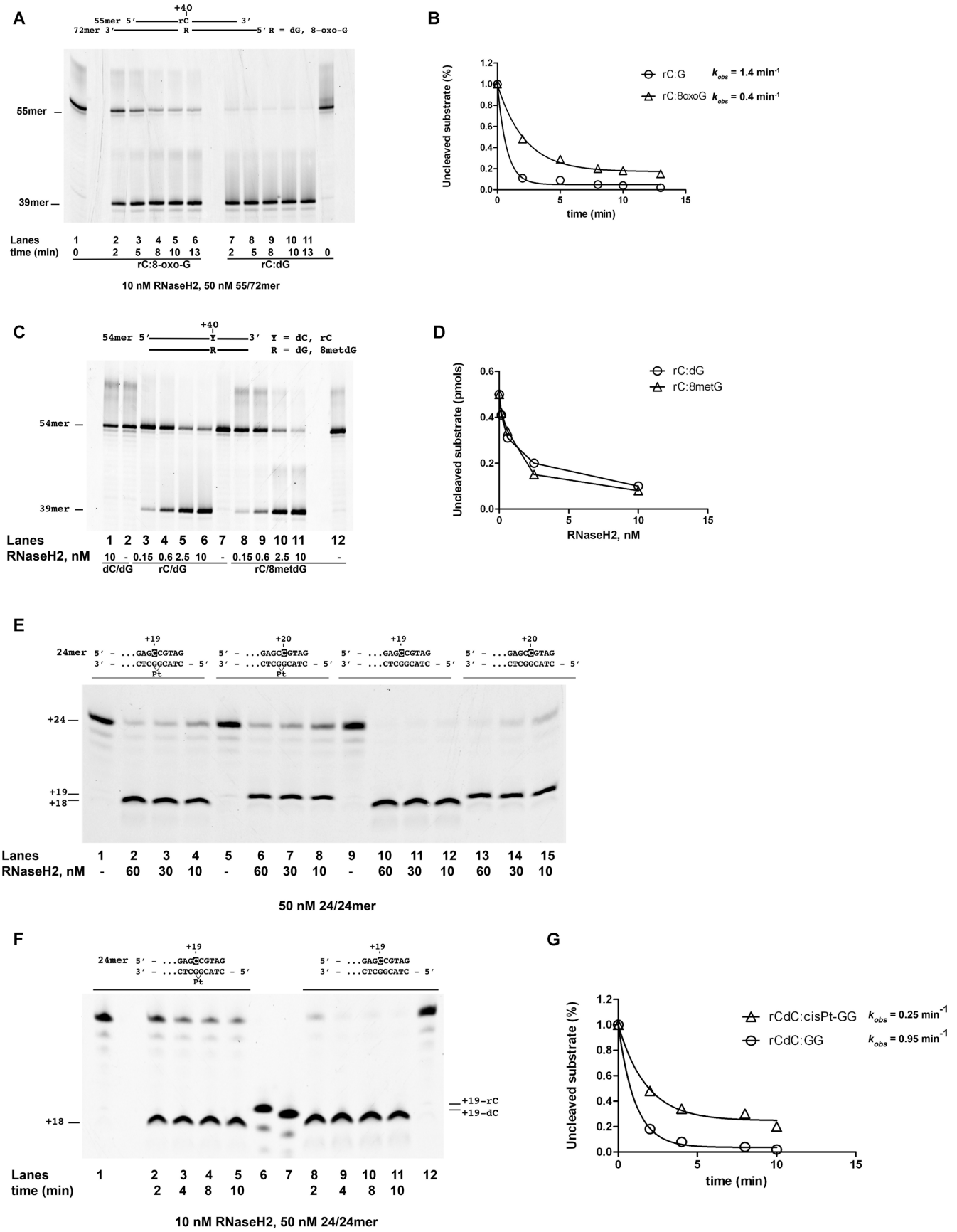

Figure 5. Cleavage of rCMP opposite normal or damaged guanines by human RNase H2. The 5′ FAM-labeled templates used are indicated on top of each panel. Asterisks indicate the labeled strands. (**A**) Time course of RNase H2 digestion of the DNA substrate containing a single rCMP opposite 8-oxo-G

and H1. In the next replication round, these RNA tracts will require Pol ζ for TLS.

Our results show that Pol η can bypass only certain lesions using rNMPs. It can easily perform TLS incorporating rCMP past a 8-oxo-G or 8-met-G, but not past 3-met-C or an AP site. Also, the nature of the lesion can influence its sugar selectivity. While the dCMP versus rCMP preference for incorporation opposite 8-met-G was similar to the one opposite a normal guanine (693 versus 400, respectively, Table 1), selectivity of dCMP opposite 8-oxo-G increased to a value of about 1400 (Table 1). Also, the fidelity of 8-oxo-G bypass was increased: the preference for rCMP versus rAMP incorporation was 8.9, while the one for dCMP versus dAMP was 3.3 (Table 1). A recent study, appearing during the preparation of this manuscript, found a similar increase in fidelity for the bypass of 8-oxo-G by human Pol η (17).

The 8-Met-G is an major alkylation product of deoxyguanosine and has miscoding properties (41). No human glycosylase has been identified so far, that can remove this lesion (42). Thus, its tolerance may rely principally on the TLS pathway. However, the capacity of human Pols to perform TLS over 8-met-G remains largely unknown. Interestingly, this modification occurs at the same position of the purine ring as in the 8-oxo-G, giving us the opportunity to compare the effects of two different substituents at the C-8 of the guanine. We found that Pol η can easily misincorporate different dNMPs opposite 8-met-G, while the complementary rCMP was the only rNMP inserted opposite this lesion. Efficient elongation past 8-met-G was observed with both dNMP and rNMP insertion. To the best of our knowledge, this is the first report of bypass of 8-met-G by a human TLS Pol.

Another important role for Pol η is in resistance toward the anticancer drug cis-Pt, which causes inter- or intrastrand crosslinks of two adjacent purines, in most cases guanines. These crosslinks block replication fork progression, requiring bypass by a specialized TLS Pol. The most frequent intrastrand crosslink is the cis-PtGG lesion. Among human Pols, Pol η has been shown to be the most proficient in bypassing cis-PtGG lesions (36). Accordingly, cells lacking Pol η, are hypersensitive to cis-Pt treatment (43,44). In cancer cells, Pol η overexpression is induced by cis-Pt treatment and its levels correlate with chemoresistance and poor clinical outcomes of several tumors, such as non-small-lung or ovarian cancers (44,45).

We found that human Pol η bypasses a cis-PtGG intrastrand crosslink by incorporating rCMP opposite the 3′-G of the lesion, then completing the bypass by incorporating dCMP opposite the 5′-G of the lesion. No rCMP incorporation could be observed opposite the 5′-G, either starting from a rCMP- or a dCMP-terminated primer. Crystal structures of Pol η in complex with a cis-PtGG and an incoming dCTP (46–48) clearly shows that incorporation opposite the 5′-G requires structural rearrangements to adsorb the 30° roll imposed by the crosslink between the two guanines. As a result, the 5′-G of the adduct can adopt either an inactive 'open' conformation or a catalytically active 'stacked' conformation. Even in the stacked conformation, the distance between the 3′-OH and the α-phosphate of the incoming dCTP poised for insertion opposite the 5′-G, is increased with respect to the complex formed with the 3′-G as the templating base, further decreasing the catalytic rate. Thus, it is possible that the presence of a 2′-OH group in the sugar of the incoming nucleotide cannot be accommodated opposite the 5′-G in the stacked conformation.

The rNMPs incorporated into the genome can be removed by RNase H2. However, very little is known about the ability of human RNase H2 in processing rNMPs incorporated opposite DNA lesions. Human RNase H2 is a heterotrimer composed of the H2A subunit that contains the catalytic site and the H2B and H2C subunits, which contribute essential structural roles (49,50). H2B also interacts with PCNA (31), which is important for the recruitment of the RNase H2 heterotrimer to DNA repair sites (51). RNase H2 knockout mice show embryonic lethality (52,53), while mutations in the RNase H2 subunits are linked to human diseases such as the Aicardi-Goutieres Syndrome (AGS) (54) and Systemic Lupus Erythematosus (SLE) (55). Thus, alterations in the catalytic efficiency of RNase H2, leading to rNMP accumulation, can have important physiological consequences (56).

We observed that human RNase H2 processes rNMPs paired to their complementary dNMPs with preference in the order rA>rU>rC>rG. The reasons for such a preference are not clear. The available crystal structures of mammalian RNase H2 enzymes (57,58) were not solved in complex with a nucleic acid substrate. However, the structure of the enzyme-substrate complex of *Thermotoga maritima* RNase H2 (59) shows that for the DNA/RNA junction, cleavage requires structural rearrangement of the sugar-phosphate backbone with rotation of the phosphodiester bond. It is tempting to speculate that such local backbone distortion my be energetically less favoured when the rNMP to be cleaved is part of a more stable rC:dG or rG:dC pair relative to rA:dT or rU:dA. Overall, these results suggest that besides the preferential incorporation of rCMP and dGMP by replicative Pols, also the lower efficiency of their removal by RNase H2 may contribute to the observed preferential accumulation of these two rNMPs in the genome.

We also observed a different preference of RNase H2 in the removal of rCMP opposite DNA lesions. A rCMP op-

←

(lanes 1–6) or undamaged guanine (lanes 7–12). (**B**) Quantification of the experiment shown in panel A. Data points were fitted to the simple exponential ([substrate]/[substrate+ product]) = $e^{-k_{obs}t}$. (**C**) RNase H2 was titrated in the presence of the DNA substrate containing a single rCMP opposite an undamaged guanine (lanes 3–6) or opposite a 8-met-G lesion (lanes 8–11). Lanes 7, 12, control reactions in the absence of enzyme. Lanes 1, 2, control reactions with the DNA substrate bearing a dCMP opposite guanine with or without enzyme, respectively. (**D**) Quantification of the experiment shown in panel C. No curve fitting was applied. (**E**) RNase H2 was titrated in the presence of the DNA substrate containing a single rCMP opposite either the 3' G (lanes 1 - 4) or the 5' G (lanes 5 - 8) of a cis-PtGG lesion (lanes 1 – 8) or the same guanines in an undamaged template (lanes 9–15). (**F**) Time course of RNase H2 digestion of the DNA substrate containing a single rCMP opposite the 3′-G of a cis-PtGG lesion (lanes 1 – 10) or the same guanine in an undamaged template (lanes 8–12) Lanes 6, 7, rCMP- and dCMP-terminated 19mer oligonucleotides, respectively, as markers. (**G**) Quantification of the experiment shown in panel E. Data points were fitted to the simple exponential ([substrate]/[substrate + product]) = $e^{-k_{obs}t}$.

Table 3. Theoretical rCMP versus dCMP incorporation frequencies opposite normal and modified G by Pol η in different cell types

Tissue	rCTP/dCTP ratio	Template G f(rCTP/dCTP)[c] × 10^{-3}	Template 8-oxo-G f(rCTP/dCTP)[c] × 10^{-3}	Template cisPt-GG f(rCTP/dCTP)[c] × 10^{-3}	Template 8metG f(rCTP/dCTP)[c] × 10^{-3}
Skin fibroblasts[a]	18	45	12	15	26
Lymphocytes[b]	200	500	140	165	288
Liver[b]	36	86	24	27	49

[a]The rCTP and dCTP concentrations have been taken from (64).
[b]The rCTP and dCTP concentrations have been taken from (63).
[c]Frequencies of incorporation for each ribo-/deoxy-nucleoside substrate pair were calculated according to the Cornish-Bowden relationship: $f(\text{rCTP/dCTP}) = (k\text{cat}/K_M)_{\text{rCTP}}/(k\text{cat}/K_M)_{\text{dCTP}} \bullet [\text{rCTP}]/[\text{dCTP}]$ using the values from Table 1 and (63,64).

posite 8-met-G was processed with the same efficiency as opposite a normal guanine, while a substantial drop in efficiency was observed when rCMP was opposite an 8–oxo-G or the 3′-G of a cis-PtGG lesion. Intriguingly, this order of preference is paralleled by Pol η, with incorporation of rCMP opposite 8-met-G being more favoured with respect to opposite 8-oxo-G or cisPt-GG. Thus, the increased probability of rCMP incorporation opposite 8-met-G may be compensated by a higher efficiency of its removal by RNase H2. On the contrary, incorporation of rCMP opposite 8-oxo-G or cis-PtGG may lead to a substantial delay in their processing by RNase H2.

Auxiliary proteins can also influence rNMPs incorporation during TLS. In this context, PCNA has been shown to interact with both Pol η and RNase H2 and to recruit both proteins at DNA repair foci (31,51,60). We did not find any stimulation of rNMP incorporation by Pol η or of rNMP cleavage by RNase H2 with PCNA. PolDIP2 is another recently identified auxiliary protein, which has been shown to stimulate the activity of Pols λ and η (28) and PrimPol (61). When tested in our system, PolDIp2 was able to significantly stimulate rNMP incorporation by Pol η on both undamaged DNA and during TLS of 8-oxo-G, 8-met-G and cis-PtGG.

In summary, the data presented here add novel details to the complex emerging picture of the consequences of rNMP incorporation during DNA repair. When considered in the context of recent data obtained for Pols λ and β (16), these results show that at least three key elements must cooperate in determining the consequences of TLS with rNMPs: (i) the intrinsic sugar selectivity of Pols (e.g. Pol λ, β or η); (ii) the relative Pol levels and/or their selective access to the lesion and (iii) the action of auxiliary proteins (e.g. PolDIp2). For example, while Pol η has lower sugar selectivity for dCMP versus rCMP incorporation opposite 8-oxo-G than Pols λ and β, experiments with cell extracts clearly indicate that the majority of rCMP insertion opposite the lesion is carried out by the more abundantly expressed Pol β (16), which can effectively compete with Pols λ and η for access to this lesion. On the other hand, the specificity of Pol η for TLS over the cis-PtGG adduct, makes rNMPs incorporation opposite this lesion almost exclusively dependent on the selectivity of this Pol. The auxiliary factor PolDIP2 can also further modulate the frequency of rNMP incorporation during TLS by Pol η. PCNA can functionally interact with both Pol η and PolDIP2 (28,62). Our *in vitro* data suggest the possibility that Pol η and PCNA may compete for their binding to PolDIP2 in a mutually exclusive way, an observation that deserves further investigations.

In turn, the complex lesions generated as a result of rNMP incorporation opposite damaged bases may impact DNA repair in two ways. First, they can affect the action of specialized DNA glycosylases, as shown in the case of the 8-oxo-G lesion, (16). In this context, the present data indicate that Pol η, similarly to Pols λ and β, has been shaped by evolution to minimize the risk of inserting rAMP opposite the lesion, which would represent the most dangerous situation, due to the poor ability of the DNA glycosylase MUTYH to process the resulting mispair (16).

Second, the novel information presented here, also clearly indicates that insertion of rNMPs opposite different lesions can reduce the efficiency of their removal by RNase H2, thus effectively delaying RER. However, RNase H2 is still able to correctly process a rNMP paired to a damaged base, albeit at a reduced rate, depending on the lesion. This indicates that the cell is still able to resolve the complex damage resulting from incorporating rNMPs during TLS. Thus, while this event may potentially cause replication stress, delaying the action of RNase H2 may also give more time for the excision repair systems to remove lesions opposite the rNMPs, which then could be efficiently addressed by RER once the complementary DNA strand is freed from the damaged bases. Finally, the findings reported here also suggest a potential role of Pol η in synthesizing long stretches of RNA. As shown in Table 3 for the case of rCMP incorporation, the theoretical frequencies of rNMPs versus dNMPs incorporation by Pol η are higher for undamaged G, than for all the three lesions considered here (8-oxo-G, cisPt-GG and 8-met-G), ranging from 4 to 50%, depending on the particular cell type (63,64). Intracellular dCTP concentrations measured in normal tissues are generally comprised between 0.3 and 30 μM, while rCTP concentrations range between 15 and 400 μM (63). However, other nucleotides show much higher differences, most notably rGTP and rATP, with respect to their corresponding dNTPs (64). Thus, depending on the cellular context, synthesis of long RNA stretches by Pol η may increase the toxicological consequences of rNMP incorporation in cells lacking RNase H2, for example in AGS patients.

SUPPLEMENTARY DATA

Supplementary Data are available at NAR Online.

FUNDING

Italian Association of Cancer Research AIRC Grant [IG15868 to G.M]; AIRC StartUP [12710 to S.S.]; University of Zurich and Swiss National Science Foundation Grant [152621 to B.v.L.]; Swiss National Science Foundation [156280]; ETH Research Commission [ETH-43 14-1 to S.J.S.]. Funding for open access charge: Italian Association of Cancer Research AIRC Grant [IG15868].
Conflict of interest statement. None declared.

REFERENCES

1. Nick McElhinny,S.A., Watts,B.E., Kumar,D., Watt,D.L., Lundstrom,E.B., Burgers,P.M., Johansson,E., Chabes,A. and Kunkel,T.A. (2010) Abundant ribonucleotide incorporation into DNA by yeast replicative polymerases. *Proc. Natl. Acad. Sci. U.S.A.*, **107**, 4949–4954.
2. Caldecott,K.W. (2014) Molecular biology. Ribose–an internal threat to DNA. *Science*, **343**, 260–261.
3. Cerritelli,S.M. and Crouch,R.J. (2016) The balancing act of ribonucleotides in DNA. *Trends Biochem. Sci.*, **41**, 434–445.
4. Williams,J.S., Lujan,S.A. and Kunkel,T.A. (2016) Processing ribonucleotides incorporated during eukaryotic DNA replication. *Nat. Rev. Mol. Cell Biol.*, **17**, 350–363.
5. Clausen,A.R., Lujan,S.A., Burkholder,A.B., Orebaugh,C.D., Williams,J.S., Clausen,M.F., Malc,E.P., Mieczkowski,P.A., Fargo,D.C., Smith,D.J. *et al.* (2015) Tracking replication enzymology in vivo by genome-wide mapping of ribonucleotide incorporation. *Nat. Struct. Mol. Biol.*, **22**, 185–191.
6. Ding,J., Taylor,M.S., Jackson,A.P. and Reijns,M.A. (2015) Genome-wide mapping of embedded ribonucleotides and other noncanonical nucleotides using emRiboSeq and EndoSeq. *Nat. Protoc.*, **10**, 1433–1444.
7. Keszthelyi,A., Daigaku,Y., Ptasinska,K., Miyabe,I. and Carr,A.M. (2015) Mapping ribonucleotides in genomic DNA and exploring replication dynamics by polymerase usage sequencing (Pu-seq). *Nat. Protoc.*, **10**, 1786–1801.
8. Bergoglio,V., Ferrari,E., Hubscher,U., Cazaux,C. and Hoffmann,J.S. (2003) DNA polymerase beta can incorporate ribonucleotides during DNA synthesis of undamaged and CPD-damaged DNA. *J. Mol. Biol.*, **331**, 1017–1023.
9. Nick McElhinny,S.A. and Ramsden,D.A. (2003) Polymerase mu is a DNA-directed DNA/RNA polymerase. *Mol. Cell. Biol.*, **23**, 2309–2315.
10. Ruiz,J.F., Juarez,R., Garcia-Diaz,M., Terrados,G., Picher,A.J., Gonzalez-Barrera,S., Fernandez de Henestrosa,A.R. and Blanco,L. (2003) Lack of sugar discrimination by human Pol mu requires a single glycine residue. *Nucleic Acids Res.*, **31**, 4441–4449.
11. Cavanaugh,N.A., Beard,W.A. and Wilson,S.H. (2010) DNA polymerase beta ribonucleotide discrimination: insertion, misinsertion, extension, and coding. *J. Biol. Chem.*, **285**, 24457–24465.
12. Gosavi,R.A., Moon,A.F., Kunkel,T.A., Pedersen,L.C. and Bebenek,K. (2012) The catalytic cycle for ribonucleotide incorporation by human DNA Pol lambda. *Nucleic Acids Res.*, **40**, 7518–7527.
13. Martin,M.J., Garcia-Ortiz,M.V., Esteban,V. and Blanco,L. (2013) Ribonucleotides and manganese ions improve non-homologous end joining by human Polmu. *Nucleic Acids Res.*, **41**, 2428–2436.
14. Donigan,K.A., McLenigan,M.P., Yang,W., Goodman,M.F. and Woodgate,R. (2014) The steric gate of DNA polymerase iota regulates ribonucleotide incorporation and deoxyribonucleotide fidelity. *J. Biol. Chem.*, **289**, 9136–9145.
15. Makarova,A.V., Nick McElhinny,S.A., Watts,B.E., Kunkel,T.A. and Burgers,P.M. (2014) Ribonucleotide incorporation by yeast DNA polymerase zeta. *DNA Rep.*, **18**, 63–67.
16. Crespan,E., Furrer,A., Rosinger,M., Bertoletti,F., Mentegari,E., Chiapparini,G., Imhof,R., Ziegler,N., Sturla,S.J., Hubscher,U. *et al.* (2016) Impact of ribonucleotide incorporation by DNA polymerases beta and lambda on oxidative base excision repair. *Nat. Commun.*, **7**, 10805.
17. Su,Y., Egli,M. and Guengerich,F.P. (2016) Mechanism of ribonucleotide incorporation by human DNA polymerase eta. *J. Biol. Chem.*, **291**, 3747–3756.
18. Cilli,P., Minoprio,A., Bossa,C., Bignami,M. and Mazzei,F. (2015) Formation and Repair of Mismatches Containing Ribonucleotides and Oxidized Bases at Repeated DNA Sequences. *J. Biol. Chem.*, **290**, 26259–26269.
19. Hubscher,U., Maga,G. and Spadari,S. (2002) Eukaryotic DNA polymerases. *Annu. Rev. Biochem.*, **71**, 133–163.
20. Hubscher,U. and Maga,G. (2011) DNA replication and repair bypass machines. *Curr. Opin. Chem. Biol.*, **15**, 627–635.
21. Donigan,K.A., Cerritelli,S.M., McDonald,J.P., Vaisman,A., Crouch,R.J. and Woodgate,R. (2015) Unlocking the steric gate of DNA polymerase eta leads to increased genomic instability in Saccharomyces cerevisiae. *DNA Rep.*, **35**, 1–12.
22. Prakash,S., Johnson,R.E. and Prakash,L. (2005) Eukaryotic translesion synthesis DNA polymerases: specificity of structure and function. *Annu. Rev. Biochem.*, **74**, 317–353.
23. Yang,W. (2014) An overview of Y-Family DNA polymerases and a case study of human DNA polymerase eta. *Biochemistry*, **53**, 2793–2803.
24. Rydberg,B. and Game,J. (2002) Excision of misincorporated ribonucleotides in DNA by RNase H (type 2) and FEN-1 in cell-free extracts. *Proc. Natl. Acad. Sci. U.S.A.*, **99**, 16654–16659.
25. Sparks,J.L., Chon,H., Cerritelli,S.M., Kunkel,T.A., Johansson,E., Crouch,R.J. and Burgers,P.M. (2012) RNase H2-initiated ribonucleotide excision repair. *Mol. Cell*, **47**, 980–986.
26. Vaisman,A. and Woodgate,R. (2015) Redundancy in ribonucleotide excision repair: Competition, compensation, and cooperation. *DNA Rep.*, **29**, 74–82.
27. Sastre-Moreno,G., Sanchez,A., Esteban,V. and Blanco,L. (2014) ATP insertion opposite 8-oxo-deoxyguanosine by Pol4 mediates error-free tolerance in Schizosaccharomyces pombe. *Nucleic Acids Res.*, **42**, 9821–9837.
28. Maga,G., Crespan,E., Markkanen,E., Imhof,R., Furrer,A., Villani,G., Hubscher,U. and van Loon,B. (2013) DNA polymerase delta-interacting protein 2 is a processivity factor for DNA polymerase lambda during 8-oxo-7,8-dihydroguanine bypass. *Proc. Natl. Acad. Sci. U.S.A.*, **110**, 18850–18855.
29. Nilforoushan,A., Furrer,A., Wyss,L.A., van Loon,B. and Sturla,S.J. (2015) Nucleotides with altered hydrogen bonding capacities impede human DNA polymerase eta by reducing synthesis in the presence of the major cisplatin DNA adduct. *J. Am. Chem. Soc.*, **137**, 4728–4734.
30. Frank,E.G., McDonald,J.P., Karata,K., Huston,D. and Woodgate,R. (2012) A strategy for the expression of recombinant proteins traditionally hard to purify. *Anal. Biochem.*, **429**, 132–139.
31. Chon,H., Vassilev,A., DePamphilis,M.L., Zhao,Y., Zhang,J., Burgers,P.M., Crouch,R.J. and Cerritelli,S.M. (2009) Contributions of the two accessory subunits, RNASEH2B and RNASEH2C, to the activity and properties of the human RNase H2 complex. *Nucleic Acids Res.*, **37**, 96–110.
32. Kannouche,P., Broughton,B.C., Volker,M., Hanaoka,F., Mullenders,L.H. and Lehmann,A.R. (2001) Domain structure, localization, and function of DNA polymerase eta, defective in xeroderma pigmentosum variant cells. *Genes Dev.*, **15**, 158–172.
33. Bienko,M., Green,C.M., Sabbioneda,S., Crosetto,N., Matic,I., Hibbert,R.G., Begovic,T., Niimi,A., Mann,M., Lehmann,A.R. *et al.* (2010) Regulation of translesion synthesis DNA polymerase eta by monoubiquitination. *Mol Cell*, **37**, 396–407.
34. Furrer,A. and van Loon,B. (2014) Handling the 3-methylcytosine lesion by six human DNA polymerases members of the B-, X- and Y-families. *Nucleic Acids Res.*, **42**, 553–566.
35. Washington,M.T., Prakash,L. and Prakash,S. (2001) Yeast DNA polymerase eta utilizes an induced-fit mechanism of nucleotide incorporation. *Cell*, **107**, 917–927.
36. Vaisman,A., Masutani,C., Hanaoka,F. and Chaney,S.G. (2000) Efficient translesion replication past oxaliplatin and cisplatin GpG adducts by human DNA polymerase eta. *Biochemistry*, **39**, 4575–4580.
37. Eder,P.S., Walder,R.Y. and Walder,J.A. (1993) Substrate specificity of human RNase H1 and its role in excision repair of ribose residues misincorporated in DNA. *Biochimie*, **75**, 123–126.
38. Lazzaro,F., Novarina,D., Amara,F., Watt,D.L., Stone,J.E., Costanzo,V., Burgers,P.M., Kunkel,T.A., Plevani,P. and

Muzi-Falconi,M. (2012) RNase H and postreplication repair protect cells from ribonucleotides incorporated in DNA. *Mol. Cell*, **45**, 99–110.
39. Clausen,A.R., Zhang,S., Burgers,P.M., Lee,M.Y. and Kunkel,T.A. (2013) Ribonucleotide incorporation, proofreading and bypass by human DNA polymerase delta. *DNA Rep.*, **12**, 121–127.
40. Clausen,A.R., Murray,M.S., Passer,A.R., Pedersen,L.C. and Kunkel,T.A. (2013) Structure-function analysis of ribonucleotide bypass by B family DNA replicases. *Proc. Natl. Acad. Sci. U.S.A.*, **110**, 16802–16807.
41. Kohda,K., Tsunomoto,H., Minoura,Y., Tanabe,K. and Shibutani,S. (1996) Synthesis, miscoding specificity, and thermodynamic stability of oligodeoxynucleotide containing 8-methyl-2'-deoxyguanosine. *Chem. Res. Toxicol.*, **9**, 1278–1284.
42. Gasparutto,D., Dherin,C., Boiteux,S. and Cadet,J. (2002) Excision of 8-methylguanine site-specifically incorporated into oligonucleotide substrates by the AlkA protein of Escherichia coli. *DNA Rep.*, **1**, 437–447.
43. Albertella,M.R., Green,C.M., Lehmann,A.R. and O'Connor,M.J. (2005) A role for polymerase eta in the cellular tolerance to cisplatin-induced damage. *Cancer Res.*, **65**, 9799–9806.
44. Chen,Y.W., Cleaver,J.E., Hanaoka,F., Chang,C.F. and Chou,K.M. (2006) A novel role of DNA polymerase eta in modulating cellular sensitivity to chemotherapeutic agents. *Mol. Cancer Res.*, **4**, 257–265.
45. Srivastava,A.K., Han,C., Zhao,R., Cui,T., Dai,Y., Mao,C., Zhao,W., Zhang,X., Yu,J. and Wang,Q.E. (2015) Enhanced expression of DNA polymerase eta contributes to cisplatin resistance of ovarian cancer stem cells. *Proc. Natl. Acad. Sci. U.S.A.*, **112**, 4411–4416.
46. Alt,A., Lammens,K., Chiocchini,C., Lammens,A., Pieck,J.C., Kuch,D., Hopfner,K.P. and Carell,T. (2007) Bypass of DNA lesions generated during anticancer treatment with cisplatin by DNA polymerase eta. *Science*, **318**, 967–970.
47. Ummat,A., Rechkoblit,O., Jain,R., Roy Choudhury,J., Johnson,R.E., Silverstein,T.D., Buku,A., Lone,S., Prakash,L., Prakash,S. *et al.* (2012) Structural basis for cisplatin DNA damage tolerance by human polymerase eta during cancer chemotherapy. *Nat. Struct. Mol. Biol.*, **19**, 628–632.
48. Zhao,Y., Biertumpfel,C., Gregory,M.T., Hua,Y.J., Hanaoka,F. and Yang,W. (2012) Structural basis of human DNA polymerase eta-mediated chemoresistance to cisplatin. *Proc. Natl. Acad. Sci. U.S.A.*, **109**, 7269–7274.
49. Cerritelli,S.M. and Crouch,R.J. (2009) Ribonuclease H: the enzymes in eukaryotes. *FEBS J.*, **276**, 1494–1505.
50. Reijns,M.A., Bubeck,D., Gibson,L.C., Graham,S.C., Baillie,G.S., Jones,E.Y. and Jackson,A.P. (2011) The structure of the human RNase H2 complex defines key interaction interfaces relevant to enzyme function and human disease. *J. Biol. Chem.*, **286**, 10530–10539.
51. Bubeck,D., Reijns,M.A., Graham,S.C., Astell,K.R., Jones,E.Y. and Jackson,A.P. (2011) PCNA directs type 2 RNase H activity on DNA replication and repair substrates. *Nucleic Acids Res.*, **39**, 3652–3666.
52. Hiller,B., Achleitner,M., Glage,S., Naumann,R., Behrendt,R. and Roers,A. (2012) Mammalian RNase H2 removes ribonucleotides from DNA to maintain genome integrity. *J. Exp. Med.*, **209**, 1419–1426.
53. Reijns,M.A., Rabe,B., Rigby,R.E., Mill,P., Astell,K.R., Lettice,L.A., Boyle,S., Leitch,A., Keighren,M., Kilanowski,F. *et al.* (2012) Enzymatic removal of ribonucleotides from DNA is essential for mammalian genome integrity and development. *Cell*, **149**, 1008–1022.
54. Crow,Y.J., Leitch,A., Hayward,B.E., Garner,A., Parmar,R., Griffith,E., Ali,M., Semple,C., Aicardi,J., Babul-Hirji,R. *et al.* (2006) Mutations in genes encoding ribonuclease H2 subunits cause Aicardi-Goutieres syndrome and mimic congenital viral brain infection. *Nat. Genet.*, **38**, 910–916.
55. Gunther,C., Kind,B., Reijns,M.A., Berndt,N., Martinez-Bueno,M., Wolf,C., Tungler,V., Chara,O., Lee,Y.A., Hubner,N. *et al.* (2015) Defective removal of ribonucleotides from DNA promotes systemic autoimmunity. *J. Clin. Invest.*, **125**, 413–424.
56. Pizzi,S., Sertic,S., Orcesi,S., Cereda,C., Bianchi,M., Jackson,A.P., Lazzaro,F., Plevani,P. and Muzi-Falconi,M. (2015) Reduction of hRNase H2 activity in Aicardi-Goutieres syndrome cells leads to replication stress and genome instability. *Hum. Mol. Gen.*, **24**, 649–658.
57. Shaban,N.M., Harvey,S., Perrino,F.W. and Hollis,T. (2010) The structure of the mammalian RNase H2 complex provides insight into RNA.NA hybrid processing to prevent immune dysfunction. *J. Biol. Chem.*, **285**, 3617–3624.
58. Figiel,M., Chon,H., Cerritelli,S.M., Cybulska,M., Crouch,R.J. and Nowotny,M. (2011) The structural and biochemical characterization of human RNase H2 complex reveals the molecular basis for substrate recognition and Aicardi-Goutieres syndrome defects. *J. Biol. Chem.*, **286**, 10540–10550.
59. Rychlik,M.P., Chon,H., Cerritelli,S.M., Klimek,P., Crouch,R.J. and Nowotny,M. (2010) Crystal structures of RNase H2 in complex with nucleic acid reveal the mechanism of RNA-DNA junction recognition and cleavage. *Mol. Cell*, **40**, 658–670.
60. Kannouche,P.L., Wing,J. and Lehmann,A.R. (2004) Interaction of human DNA polymerase eta with monoubiquitinated PCNA: a possible mechanism for the polymerase switch in response to DNA damage. *Mol. Cell*, **14**, 491–500.
61. Guilliam,T.A., Bailey,L.J., Brissett,N.C. and Doherty,A.J. (2016) PolDIP2 interacts with human PrimPol and enhances its DNA polymerase activities. *Nucleic Acids Res.*, **44**, 3317–3329.
62. Tissier,A., Janel-Bintz,R., Coulon,S., Klaile,E., Kannouche,P., Fuchs,R. P. and Cordonnier,A. M. (2010) Crosstalk between replicative and translesional DNA polymerases: PDIP38 interacts directly with Pol eta *DNA Repair (Amst)* **9**, 922–928.
63. Traut,T.W. (1994) Physiological concentrations of purines and pyrimidines. *Mol. Cell. Biochem.*, **140**, 1–22.
64. Ferraro,P., Franzolin,E., Pontarin,G., Reichard,P. and Bianchi,V. (2010) Quantitation of cellular deoxynucleoside triphosphates. *Nucleic Acids Res*, **38**, e85.